Anharmonicity on Al(100) and Al(111) surfaces

R. Zivieri, G. Santoro, and V. Bortolani
Dipartimento di Fisica and INFM Unità di Ricerca di Modena, Università degli Studi di Modena, Via Campi 213/A, I-41100 Modena, Italy
(Received 12 November 1998)

We present a molecular-dynamics analysis of the stable nonmelting (100) and (111) surfaces of Al. A many-body potential derived from first-principles calculations is used. The molecular-dynamics method includes anharmonic effects of all orders. We study static and dynamical properties of the surface. An expansion of the (111) surface and a contraction of the (100) surface results from the calculations. At low temperature, the vertical mean-square vibrational amplitude is larger than the in-plane component, while at higher temperature the in-plane component approaches the vertical one. Both components are at least twice as large as the bulk value. The interactions due to the surface decay very rapidly going into the crystal from the surface, as indicated by the analysis of the Debye-Waller factor. The evaluated linewidths for the Rayleigh surface phonon reproduce quite well the temperature dependence of the He-surface scattering data. The experimental behavior of the energy shifts, as a function of the scattering momentum transfer, presents a minimum inside the Brillouin zone, which is also found by our calculations. The surface energy shifts are about 30% larger than the bulk ones at the same temperature. The effect of surface anharmonicity is much larger for the static properties than for the dynamical properties. [S0163-1829(99)05924-X]

I. INTRODUCTION

In recent years there has been considerable interest in the experimental and theoretical study of anharmonic properties of single-crystal surfaces. Anharmonicity is responsible for important surface processes, such as thermal expansion,[1,2] reconstructive phase transitions,[3] roughening,[4] and surface melting,[5] as well as Debye-Waller effects.[6,7] It has been shown that the open surface (110) of several metals exhibits surface melting,[8–14] while the close-packed (100) and (111) surfaces are stable up to the bulk melting point.[11,15] Static displacements associated with the relaxation of the surface plane were obtained with low-energy electron diffraction[16] (LEED) and Mev ion-scattering techniques.[17] Measurements performed with helium-atom-scattering [18] (HAS) were able to resolve the energy shifts and the linewidths associated with one-phonon scattering processes. Several theoretical methods, such as quasiharmonic approximation,[19] perturbation theory,[20] and molecular-dynamics[21,22] (MD) have been developed to study the phonon-phonon interaction. In the perturbative approach[20] the anharmonic interaction includes third- and fourth-order terms in the phonon-phonon interaction. The MD method is not limited to an expansion of the potential in terms of the displacements and all the orders of the phonon processes are automatically summed up. For this reason, in this paper we use the MD technique to investigate the anharmonic properties of Al surfaces. The semi-infinite crystal is modeled with a slab composed by several thousands of atoms. To perform the computer simulation of the correlation functions for the slab, which involves long simulation times, we use a classical interaction potential. *Ab initio* simulations are not yet suitable for this type of calculations. We study the anharmonic properties of the close surfaces which are stable up to the melting temperature. We focus our attention on the Al(100) and Al(111) surfaces. For the Al(111) surface there has been a long controversy concerning the expansion[23–25] or the contraction[26] of the surface layer. The recent LEED measurements[16,27] report an expansion of the first two layers. Many of the theoretical studies, based on various techniques, are predicting a surface contraction. In this paper we study the surface relaxations and the Debye-Waller factors of the Al stable surfaces in order to analyze, in particular, the expansion of the (111) surface. Our second aim is the evaluation of the energy shifts and of the one-phonon linewidths, as a function of momentum transfer and temperature, to see if, in the same framework, we can explain a large set of anharmonic properties of Al surfaces. In Sec. II we discuss technical points relative to the application of MD simulations to the calculation of the static relaxations, mean-square vibrations, Debye-Waller factor, and displacement-displacement correlation functions. The results for the interlayer relaxations, mean-square displacements and Debye-Waller factor are presented for (100) and (111) surfaces in Sec. III together with a comparison of the available experimental data for a set of temperatures. Section IV is devoted to the study of the one-phonon linewidths and energy shifts for the (100) surface where a comparison is made with the He scattering data for the Rayleigh phonons. In Sec.V the conclusions are drawn.

II. SIMULATION METHOD

In order to perform the MD simulations, we use the many-body potential of Ercolessi and Adams[28] constructed in the scheme of the embedded-atom method.[29] The parameters entering in the potential are determined by fitting the total potential to *ab initio* calculations of the forces in many atomic configurations. The range of the potential extends up to third neighbors. In order to study surface properties, we consider a slab of a sufficient number of planes to avoid interactions between the two surfaces. Each plane contains a two-dimensional (2D) supercell on which we impose peri-

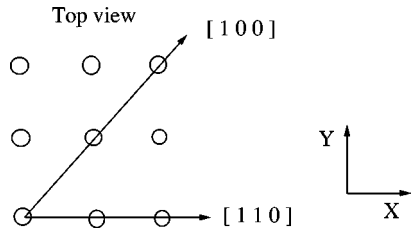

FIG. 1. The top view of the fcc (100) surface. First layer atoms are represented. The x and y axes are indicated.

odic boundary conditions in the two directions parallel to the surface. The Al(100) surface is modeled by a slab of 24 planes. Each layer contains 100 atoms. The Al(111) surface is represented by a slab of 20 planes. The 2D supercell contains 192 atoms. No periodic boundary conditions are imposed on the surface normal. We perform the simulation at a given T in the Andersen scheme[30] and we determine the equilibrium volume for the system under zero pressure. From this volume, we determine the surface lattice constants used as input parameters in the surface simulations. The z direction, normal to the surface, is allowed to fluctuate. We start at $T=0$ K randomizing the atomic positions and imposing zero kinetic energy on the system. We use a time step $\Delta\tau = 0.265\times10^{-14}$ s for each temperature considered. With a run of about 1000 time steps the system reaches an equilibrium configuration at $T=0$ K. Then the system is put in contact with a thermal bath at a given temperature in order to heat the crystal. A run of 1000 time steps is sufficient to reach the requested temperature. In the range of temperatures $T=100$–400 K, we continue the simulation for a total of 5000 time steps corresponding to 10 ps. For T in the range 500–700 K we perform a longer simulation of 20 ps. During this last run the instantaneous positions are stored at each time step for the analysis of the properties of the system. In this way we can evaluate

(1) the static interlayer relaxation between adjacent layers defined by

$$d_{j,j+1}=\frac{1}{N_j}\frac{1}{T}\int_0^T dt\left[\sum_{l=1}^{N_j} z^j(l,t)-\sum_{l'=1}^{N_{j+1}} z^{j+1}(l',t)\right], \quad (1)$$

where N_j is the number of atoms in each layer with $N_j = N_{j+1}$; $j=1$ corresponds to the surface layer and $j>1$ labels the layers inside the slab where j is the index of the layer considered;

(2) the vertical and in-plane mean-square displacements defined, respectively, as

TABLE I. Temperature dependence of the relaxations for the (100) surface. Interlayer distances for the first three layers are presented. The bulk values are also reported. Units are in Å.

Temp	d_{bulk}	d_{12}	Δ_{12} (%)	d_{23}	Δ_{23} (%)
130 K	2.020	1.985	−1.73	2.003	−0.84
200 K	2.023	1.994	−1.43	2.000	−1.14
300 K	2.026	1.999	−1.33	2.008	−0.89
440 K	2.030	2.007	−1.13	2.031	+0.00
500 K	2.033	2.016	−0.84	2.025	−0.39
600 K	2.037	2.026	−0.54	2.023	−0.69
700 K	2.041	2.035	−0.29	2.047	+0.29

$$\langle u_{jz}^2\rangle=\frac{1}{N_j}\frac{1}{T}\sum_l^{N_j}\int_0^T dt|\mathbf{R}_z^j(l,t)-\mathbf{R}_z^j(l)|^2, \quad (2)$$

$$\langle u_{j\|}^2\rangle=\frac{1}{N_j}\frac{1}{T}\sum_l^{N_j}\int_0^T dt(|\mathbf{R}_x^j(l,t)-\mathbf{R}_x^j(l)|^2 + |\mathbf{R}_y^j(l,t)-\mathbf{R}_y^j(l)|^2), \quad (3)$$

where $\mathbf{R}_\alpha^j(l)$ with $\alpha=x,y,z$ is the mean position of the lth atom in the jth layer and $\langle\ \rangle$ denotes the temporal average;

(3) the Debye-Waller factor[31] for the atomic layer j given by $e^{-2W(j)}$ where

$$2W(j)=\langle(\mathbf{k}\cdot\mathbf{u}_j)^2\rangle-\frac{1}{12}[\langle(\mathbf{k}\cdot\mathbf{u}_j)^4\rangle-3\langle(\mathbf{k}\cdot\mathbf{u}_j)^2\rangle^2]+\cdots, \quad (4)$$

being $\mathbf{k}$ the momentum transfer of the incident particle[31] (photon, electron, or atom). Maradudin and Fein[32] have shown that the largest anharmonic contributions to $2W$ arise from the anharmonic averaged term $\langle(\mathbf{k}\cdot\mathbf{u}_j)^2\rangle$. For this reason we will consider in $2W$ only the first term.

The time-dependent displacement-displacement autocorrelation function[33,34] is defined in the one-phonon approximation for each layer j as a tensor of the form

$$c_{\alpha\beta}^j(\mathbf{Q},t)=\lim_{T\to\infty}\frac{1}{T-t}\frac{1}{N_j}\sum_{l,l'}\int_0^{T-t} d\tau u_\alpha^j(l,t+\tau) \times u_\beta^j(l',t)e^{i\mathbf{Q}\cdot[\mathbf{R}^j(l)-\mathbf{R}^j(l')]}. \quad (5)$$

$\mathbf{Q}$ is the in-plane component of the vector $\mathbf{q}=(\mathbf{Q},q_z)$ and $\mathbf{R}^j(l)$ is the mean position of the lth atom in the jth layer. To evaluate the displacement-displacement correlation function we need a long simulation run of the order of 100 ps. We prepare the system at a given T, as described before, and we

TABLE II. Vertical and horizontal mean-square displacements on the (100) face for the first three layers as a function of temperature. Units are given in 10^{-2} Å^2.

Temp.	$\langle u_{1z}^2\rangle$	$\langle u_{1\|}^2\rangle$	$\langle u_{1z}^2\rangle/\langle u_{1\|}^2\rangle$	$\langle u_{2z}^2\rangle$	$\langle u_{2\|}^2\rangle$	$\langle u_{2z}^2\rangle/\langle u_{2\|}^2\rangle$	$\langle u_{3z}^2\rangle$	$\langle u_{3\|}^2\rangle$	$\langle u_{3z}^2\rangle/\langle u_{3\|}^2\rangle$
130 K	0.88	0.67	1.31	0.55	0.47	1.17	0.48	0.44	1.09
300 K	2.27	1.77	1.28	1.70	1.17	1.45	1.29	1.19	1.08
500 K	3.48	3.16	1.10	2.30	2.00	1.15	2.14	2.06	1.04
600 K	4.34	4.08	1.06	2.96	2.86	1.03	2.56	2.30	1.11

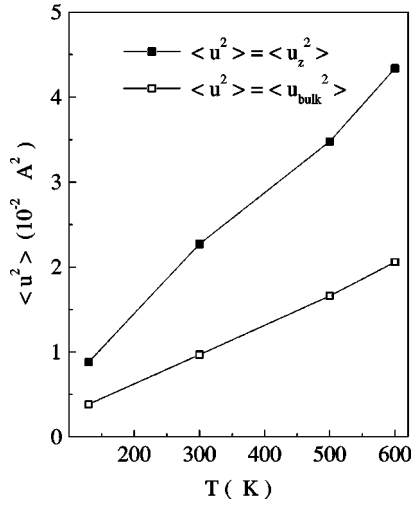

FIG. 2. Full squares: Temperature dependence of the first layer vertical mean-square displacement for the (100) surface. Open squares: Unidimensional bulk mean-square displacements.

evaluate the total energy as a mean value from the 1000 time steps run necessary to thermalize the system. Fixing the energy at this value, we perform a simulation of 50 000 time steps. The spectral density for the generic jth layer is expressed as the Fourier transform of the displacement-displacement temporal autocorrelation function and is defined,[34] in the limit of long simulation times, as

$$S^j_{\alpha\beta}(\mathbf{Q},\omega) = \lim_{T\to\infty}\frac{1}{T}\frac{1}{N_j}\int_0^T dt u^j_{\mathbf{Q}\alpha}(t)e^{i\omega t}\int_0^T dt' u^j_{-\mathbf{Q}\beta}(t')e^{-i\omega t'}, \quad (6)$$

where

$$u^j_{\mathbf{Q}\alpha}(t)=\sum_l e^{i\mathbf{Q}\cdot\mathbf{R}^j(l)}u^j_\alpha(l,t). \quad (7)$$

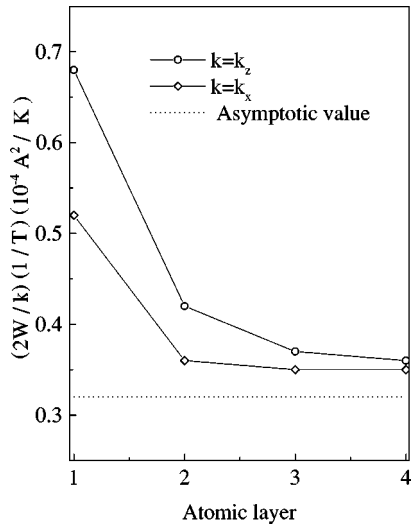

FIG. 3. Exponent of the Debye-Waller factor at $T=130$ K as a function of the atomic layers. Open circles: $\mathbf{k}=(0,0,k_z)$ with $k_z=1.56$ Å^{-1}. Full circles: The same for $\mathbf{k}=(k_x,0,0)$ with $k_x=1.56$ Å^{-1}.

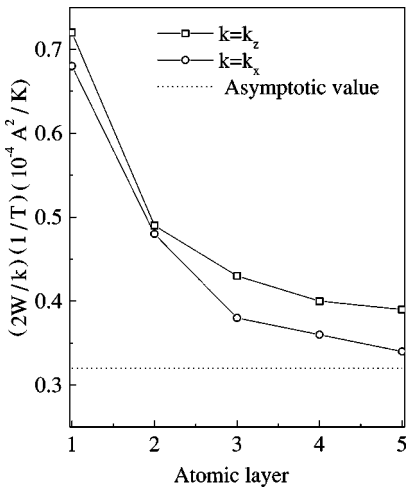

FIG. 4. As in Fig. 3 for $T=600$ K.

We remind that for an anharmonic crystal the one-phonon cross section can be very well approximated[32] by the product of the correlation function given by Eq. (5) times the Debye-Waller factor of Eq. (4).

III. INTERLAYER RELAXATIONS AND MEAN-SQUARE AMPLITUDES

We start by considering the Al(100) slab. The geometry of the Al(100) surface is shown in Fig. 1. The calculated value of the separation between first and second layer, d_{12}, second and third layer, d_{23}, and the bulk separation, d_{bulk}, are presented in Table I for several temperatures. The (100) surface contracts, as also found in the MD calculations of Yang *et al.*[22] for Cu(100). The contraction between the first and second plane, $\Delta d_{12}=(d_{12}-d_{\text{bulk}})/d_{\text{bulk}}$, decreases rapidly with increasing temperature and, at $T=700$ K, is -0.29%. We notice that there is not a general consensus[35–40] on the relaxation of the surface as a function of T. The old LEED (Refs. 23 and 41) and extended x-ray absorption measurements[26] give evidence of no contraction. Medium energy electron diffraction[42] and MeV ion scattering[17] measurements, however, give a contraction at low and at room temperature of less than 0.05 Å in agreement with our calculations. Close to the melting point Monte Carlo simulations[35] predict an outward relaxation. The second and third layer present an expansion at high temperature, shown by the positive sign of $\Delta d_{23}=(d_{23}-d_{\text{bulk}})/d_{\text{bulk}}$ at $T=700$ K. The parallel and perpendicular to the surface mean-square amplitudes of the first three layers are summarized in

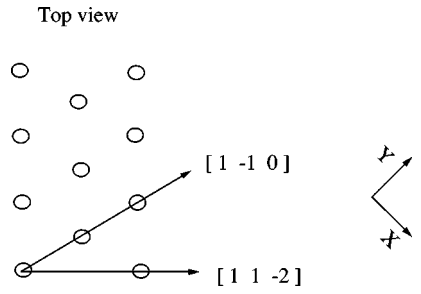

FIG. 5. The top view of the fcc (111) surface. First layer atoms are represented. The x and y axes are indicated.

TABLE III. As in Table I for the (111) surface. Experimental data at $T=90$ K from Ref. 24 and at $T=160$ K from Ref. 15.

Temp	d_{bulk}	d_{12}	Δ_{12} (%) (calc)	Δ_{12} (%) (expt.)	d_{23}	Δ_{23} (%) (calc.)	Δ_{23} (%) (expt.)
90 K	2.331	2.354	+0.90	$+0.90\pm0.5$	2.344	+0.53	+0.5
160 K	2.334	2.374	+1.71	$+1.70\pm0.3$	2.350	+0.67	$+0.5\pm0.7$
300 K	2.339	2.367	+1.20	+1.80	2.347	+0.34	+0.1
500 K	2.347	2.363	+0.68		2.344	−0.13	
600 K	2.352	2.369	+0.72		2.347	−0.21	
700 K	2.356	2.369	+0.55		2.358	+0.08	

Table II. For the (100) surface $\langle u_{jx}^2\rangle=\langle u_{jy}^2\rangle$ (see Fig. 1). At low temperature, we find an anisotropy of 30% which decreases with temperature. At 600 K the anisotropy is of less than 10%. Our MD simulation at this temperature does not indicate the presence of diffusive processes which can produce a large increase of the lateral mean-square amplitudes. In particular, the behavior of the transverse component of the surface displacement, as a function of temperature, is illustrated in Fig. 2. One notes, in the range of temperatures studied, a linear behavior for the unidimensional bulk component as well as for the transverse surface one. At low temperature the vertical mean-square displacement is twice as large as that of the bulk, but the deviation increases approximately linearly with temperature. In Table II are also reported the mean-square amplitudes of the second and third layer. As it can be noticed, there is a strong reduction of the mean-square amplitudes, which tend to the bulk values going from the surface inside the crystal. This is better illustrated in Fig. 3 where we present the Debye-Waller factor at low temperature ($T=130$ K) for the $\mathbf{k}=(k_x,0,0)$ parallel to the surface and for the $\mathbf{k}=(0,0,k_z)$ perpendicular to the surface for different atomic layers. The surface correction is larger for vibration perpendicular to the surface than for vibration parallel to the surface and decays very rapidly within a few atomic spacings from the surface. It is important to notice that this Debye-Waller behavior reproduces quite closely the results of Maradudin and Melngailis.[6] These calculations were performed by taking the Bose factor in the high-temperature limit[43] and evaluating $2W(j)$ at the lowest order in the anharmonic force constants. This correspondence indicates that, in our calculations, the three-phonon processes are the dominating ones. At high temperature ($T=600$ K), as shown in Fig. 4, higher-order phonon contributions become very important. We now turn to discuss the Al(111) surface. The geometry adopted in our calculations is presented in Fig. 5. The evaluated interlayer relaxations for the first two layers are summarized in Table III together with experimental results. We obtain an expansion of the first and second layer. In particular, at $T=90$ K the calculations are in very good agreement with experimental data[24] for both layers. Our results at $T=160$ K reproduce quite well the recent measurements of Nooan and Davis.[16] The comparison between the evaluated theoretical values and the observed ones[16] is not so good at room temperature. Nevertheless, several theories not only predict a contraction of the first layer,[36,44,45] but also that an expansion is not possible, as discussed by Finnis and Heine.[46] Finally, the mean-square displacements of our calculations are given in Table IV. For the symmetry of this surface, see Fig. 5, we have $\langle u_{jx}^2\rangle=\langle u_{jy}^2\rangle$. The anisotropy between the vertical and the horizontal component decreases with temperature, but remains larger than one. At 700 K our simulation does not indicate any considerable diffusion of the atoms in the surface plane so that the planar mean-square displacement remains smaller than the vertical one. The evaluation of the Debye-Waller factors involving the lateral and vertical mean-square displacements are rather similar to those discussed for the (100) surface and are not reported here. We stress again that, at low temperature, the mean-square displacements are mainly related to three-phonon processes. The effect of higher-order contributions is visible in the high-temperature limit.

IV. LINEWIDTHS AND ENERGY SHIFTS

Previous calculations of the linewidths for Lennard-Jones crystals were performed by McGurn *et al.*[34] Embedded-atom method calculations were performed by Ditlevsen *et al.*[47] and by Yang *et al.*[22] A MD simulation of Al was performed by Gester *et al.*[18] using a Morse potential. All these simulations indicate that the presence of the surface enhances the bulk linewidths. We start by evaluating the linewidths associated to the Rayleigh mode as a function of momentum transfer. Accurate measurements have been performed with He-surface inelastic scattering[18] (HAS) of the Rayleigh one-phonon spectra for the Al(100) surface in the Σ direction. The intensity of the Rayleigh peak strongly decreases with increasing lateral momentum; for this reason accurate measurements have been performed for lateral momentum more

TABLE IV. As in Table II for the (111) surface.

Temp.	$\langle u_{1z}^2\rangle$	$\langle u_{1\parallel}^2\rangle$	$\langle u_{1z}^2\rangle/\langle u_{1\parallel}^2\rangle$	$\langle u_{2z}^2\rangle$	$\langle u_{2\parallel}^2\rangle$	$\langle u_{2z}^2\rangle/\langle u_{2\parallel}^2\rangle$	$\langle u_{3z}^2\rangle$	$\langle u_{3\parallel}^2\rangle$	$\langle u_{3z}^2\rangle/\langle u_{3\parallel}^2\rangle$
200 K	1.21	0.70	1.73	0.88	0.65	1.35	0.68	0.57	1.20
300 K	2.04	1.29	1.58	1.60	1.18	1.36	1.10	0.98	1.12
500 K	3.22	2.13	1.51	2.20	1.80	1.22	1.83	1.73	1.06
600 K	4.31	3.22	1.34	2.81	2.29	1.23	2.46	2.25	1.09
700 K	4.59	4.55	1.01	3.77	3.29	1.15	3.39	2.74	1.24

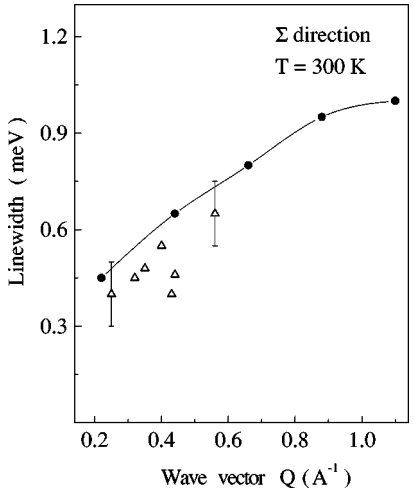

FIG. 6. Phonon linewidth of the Rayleigh mode in the Σ direction at $T=300$ K for the (100) surface. Full circles: calculated values. Triangles: experimental points from Ref. 18.

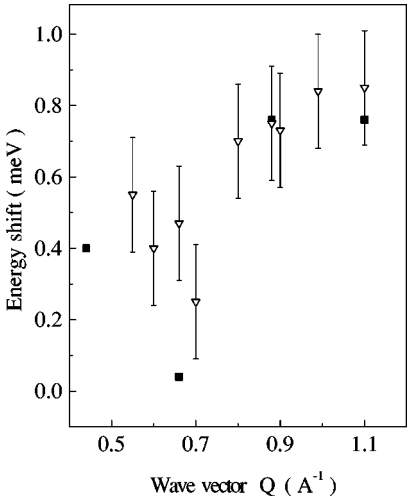

FIG. 8. Energy shift, as defined in the text, of the Rayleigh mode at $T=300$ K. Full squares: calculated values. Triangles: experimental points from Ref. 18.

than half of the zone-boundary value, where the Rayleigh peak rises well above the multiphonon background. Measurements have been performed at $T=300$ K and at $T=440$ K. In Fig. 6 we present our results at $T=300$ K. The linewidth is defined as the width at half maximum of the Rayleigh peak evaluated with Eq. (6). Our results are in good agreement with the experimental measurements. Also for the higher temperature, $T=440$ K, our simulation is in agreement with the measured linewidths, as shown in Fig. 7, and indicates that the increase in linewidth is larger than that one predicted by the use of the Morse potential.[18] Moreover, MD calculations performed with Morse potential largely underestimate at this temperature the linewidths, especially for small momentum transfer, the region where multiphonon effects are dominating and the many-body potential plays a noticeable role. We note that the surface linewidths are larger than in the bulk. The $\bar{\Gamma}\rightarrow\bar{X}$ direction is parallel to the bulk $\Gamma\rightarrow K$ direction and $\bar{X}$ corresponds to the T_2 bulk mode with momentum transfer equal to $(2\pi/a)[\frac{1}{2},\frac{1}{2},0]$. A direct comparison is not possible, because the experiments cannot be performed at $\bar{X}$. However, our surface calculations give at $\bar{X}$ a value of 1 meV at $T=300$ K, as it can be seen from Fig. 6, which is $\simeq 30\%$ larger than the bulk value previously evaluated[48] at the same temperature. This is a further indication that multiphonon effects are enhanced by the presence of the surface. We now turn to discuss the energy shifts. In order to make a stringent comparison with the experimental data we define the energy shift as $\Delta\omega=\omega_T(\mathbf{Q})-\omega_{T_m}(\mathbf{Q})$, where T_m is the lowest temperature at which the surface Rayleigh mode is measured with the HAS technique.[18] For Al(100) $T_m=130$ K. The experimental results of the Rayleigh phonon-dispersion curves are clearly separated from the background in the second half of the Brillouin zone. For this reason, we present the results only for $Q\geqslant 0.5$ Å^{-1}. In Fig. 8 are reported the experimental data together with the calculations at $T=300$ K. It can be noticed that the behavior of the energy shifts as a function of the momentum is rather similar to that one of the T_2 phonon shift in the bulk in the [110] direction even if the surface energy shifts are larger. Moreover, for the smallest **Q**, we obtain convergence in the numerical value by taking a supercell with 400 atoms in each layer. This is an indication that multiphonon processes of

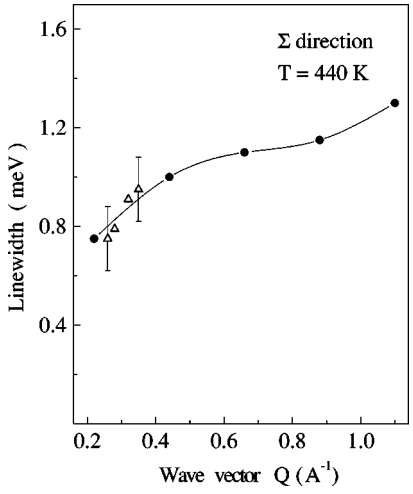

FIG. 7. As in Fig. 6 at $T=440$ K.

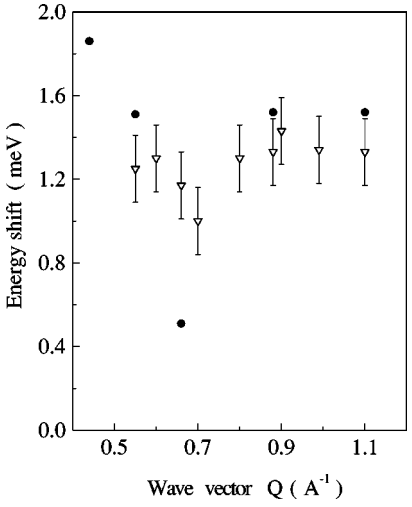

FIG. 9. As in Fig. 8 at $T=440$ K.

high order are very important, as already emphasized in the bulk calculations.[48] In Fig. 9 are presented the results for $T=440$ K. There is a noticeable increase of the energy shift, but the dip present around $\mathbf{Q}=0.7$ Å^{-1} still remains. As a function of $\mathbf{Q}$ the effect of anharmonicity is not linear. Our theoretical results reproduce the experimental trend, even if at $\mathbf{Q}=0.66$ Å^{-1} we underestimate the experimental value. If we assume a linear temperature dependence at the $\overline{X}$ point, the slope is 0.4 meV for 100 K. The slope reduces at 0.2 meV for 100 K at the smaller momentum, in agreement with the experiments of Gester *et al.*[18]

V. CONCLUSIONS

In this paper we have shown that a MD simulation based on a surface free parameter many-body potential reproduces quite accurately both static and dynamic anharmonic effects in the smooth aluminum surfaces. The evaluated properties turn out to be very sensitive to the number of particles and to the total simulation time. To get convergent results several thousands of particles are necessary. For the static properties a small simulation time of 10 ps is required to reach convergence in the calculations, whereas for the evaluation of the width of the spectral densities a larger simulation time is requested (100 ps). Our results depend on the surface orientation. We predict a small contraction of the (100) and an expansion of the (111) surface in agreement with the experiments. This is a relevant theoretical result, because many MD and *ab initio* calculations give a surface contraction. The surface mean-square displacements are, at low temperature, at least twice as much the bulk one's. The ratio increases at higher temperature. The behavior of the Debye-Waller factor in the range of temperature considered differs very slightly from the linear behavior found in earlier calculations.[6] The interactions produced by the surface decay quite rapidly going from the surface inside the slab. The fifth layer can already be considered as a bulk layer. The evaluated linewidths, as a function of the lateral momentum, reproduce in a satisfactory way the scattering data. Also the temperature behavior is quite well described by our many-body potential. Calculations performed with the Morse potential do largely underestimate the experimental linewidths. As shown in our study, the evaluated energy shifts present a nonmonotonic trend as found in the experimental data. Our analysis indicates that the presence of the surface largely enhances the anharmonic contributions of the static properties and produces only small effects in the surface dynamical properties.

ACKNOWLEDGMENT

G.S. acknowledges partial financial support from NATO, Collaborative Research Grant No. CRG971622.

[1] L. Dobrzynski and A. A. Maradudin, Phys. Rev. B **7**, 1207 (1973).
[2] Y. Cao and E. Conrad, Phys. Rev. Lett. **65**, 2808 (1990).
[3] I. K. Robinson, E. Vlieg, H. Hornis, and E. H. Conrad, Phys. Rev. Lett. **67**, 1890 (1991).
[4] G. Armand, D. Gorse, J. Lapujoulade, and J. R. Manson, Europhys. Lett. **3**, 1113 (1987).
[5] J. W. M. Frenken, P. M. J. Marée, and J. F. Van der Veen, Phys. Rev. B **34**, 7506 (1986).
[6] A. A. Maradudin and J. Melngailis, Phys. Rev. B **133**, A1188 (1964).
[7] G. Armand and J. R. Manson, Phys. Rev. Lett. **53**, 1112 (1984).
[8] P. Carnevali, F. Ercolessi, and E. Tosatti, Phys. Rev. B **36**, 6701 (1987).
[9] F. Ercolessi, S. Iarlori, O. Tomagnini, E. Tosatti, and X. J. Chen, Surf. Sci. **251/252**, 645 (1991).
[10] A. Hoss, M. Nold, P. von Blanckenhagen, and O. Meyer, Phys. Rev. B **45**, 8714 (1992).
[11] A. W. Denier van der Gon, R. J. Smith, J. M. Gay, D. J. O'Connor, and J. F. Van der Veen, Surf. Sci. **227**, 143 (1990).
[12] A. W. Denier van der Gon, D. Frenkel, J. W. M. Frenken, R. J. Smith, and P. Stolze, Surf. Sci. **256**, 385 (1991).
[13] P. Stoltze, J. K. Nørskov, and U. Landman, Phys. Rev. Lett. **61**, 440 (1988).
[14] P. Stoltze, J. K. Nørskov, and U. Landmann, Surf. Sci. Lett. **220**, L693 (1989).
[15] F. D. Di Tolla, F. Ercolessi, and E. Tosatti, Phys. Rev. Lett. **74**, 3201 (1995).
[16] J. R. Noonan and H. L. Davis, J. Vac. Sci. Technol. A **8**, 2671 (1990).
[17] C. Huan-Sheng, C. Zhi-Xiang, X. Hong-Jie, Y. Xiao-Wei, and Y. Fu-Jia, Nucl. Instrum. Methods Phys. Res. B **45**, 24 (1990).
[18] M. Gester, D. Kleinhesselink, P. Ruggerone, and J. P. Toennies, Phys. Rev. B **49**, 5777 (1994).
[19] N. R. Werthamer, *Theory of Lattice Dynamics of Rare Gas Crystals* (Academic, New York, 1973), p. 265.
[20] A. Franchini, G. Santoro, V. Bortolani, A. A. Maradudin, and R. F. Wallis, Phys. Rev. B **45**, 11 982 (1992).
[21] C. Z. Wang, A. Fasolino, and E. Tosatti, Phys. Rev. B **37**, 2116 (1988).
[22] L. Yang and T. S. Rahman, Phys. Rev. Lett. **67**, 2327 (1991); L. Yang, T. Rahman, and M. Daw, Phys. Rev. B **44**, 13 725 (1991).
[23] D. W. Jepsen, P. M. Marcus, and F. Jona, Phys. Rev. B **5**, 3933 (1972).
[24] H. B. Nielsen and D. L. Adams, J. Phys. C **15**, 615 (1982).
[25] D. W. Jepsen, P. M. Marcus, and F. Jona, Phys. Rev. B **6**, 3684 (1972).
[26] A. Bianconi and R. Z. Bachrach, Phys. Rev. Lett. **42**, 104 (1979).
[27] H. B. Nielsen and D. L. Adams, J. Phys. C **15**, 615 (1982).
[28] F. Ercolessi and J. B. Adams, Europhys. Lett. **26**, 583 (1994).
[29] M. S. Daw and M. I. Baskes, Phys. Rev. Lett. **50**, 1285 (1983); Phys. Rev. B **29**, 6443 (1984).
[30] H. C. Andersen, J. Chem. Phys. **72**, 2384 (1980).
[31] N. Garcia, A. A. Maradudin, and V. Celli, Philos. Mag. A **45**, 287 (1982); V. Celli and A. A. Maradudin, Phys. Rev. B **31**, 825 (1985).
[32] A. A. Maradudin and A. E. Fein, Phys. Rev. B **128**, 2589 (1962).
[33] J. P. Hansen and M. L. Klein, Phys. Rev. B **13**, 878 (1976); J. Phys. (Paris) **35**, L-29 (1974).
[34] A. R. McGurn, A. A. Maradudin, R. F. Wallis, and A. J. C. Ladd, Phys. Rev. B **37**, 3964 (1988).

[35] A. M. Molenbroek and J. W. M. Frenken, Phys. Rev. B **50**, 11 132 (1994).
[36] N. Ting, Y. Qingliang, and Y. Yiying, Surf. Sci. **206**, L857 (1988).
[37] T. J. Raeker and A. E. DePristo, Phys. Rev. B **39**, 9967 (1989).
[38] R. N. Barnett, U. Landman, and C. L. Cleveland, Phys. Rev. B **28**, 1685 (1983).
[39] K.-P. Bohnen and K.-M. Ho, Surf. Sci. **207**, 105 (1988).
[40] S. Debiaggi and A. Caro, J. Phys.: Condens. Matter **4**, 3905 (1992).
[41] F. Jona, D. Sondericker, and P. M. Marcus, J. Phys. C **13**, L155 (1980).
[42] N. Masud, R. Baudoing, D. Aberdam, and C. Gaubert, Surf. Sci. **133**, 580 (1983).
[43] A. A. Maradudin, P. A. Flinn, and J. M. Radcliffe, Ann. Phys. (N.Y.) **26**, 81 (1964).
[44] H. Cox, R. L. Johnston, and J. N. Murrell, Surf. Sci. **373**, 67 (1997).
[45] J. R. Smith and A. Banerjea, Phys. Rev. B **37**, 10 411 (1988).
[46] M. W. Finnis and V. Heine, J. Phys. F **4**, L37 (1974).
[47] P. D. Ditlevsen, P. Stoltze, and J. K. Nørskov, Phys. Rev. B **44**, 13 002 (1991).
[48] R. Zivieri, G. Santoro, and V. Bortolani, Phys. Rev. B **58**, 5429 (1998).